ENGINEERING JOURNAL

Fabrication of Porous Hydroxyapatite through Combination of Sacrificial Template and Direct Foaming Techniques

Sujin Woottichaiwat[1] , Somchai Puajindanetr[1,*], and Serena M. Best[2]

1 Department of Industrial Engineering, Faculty of Engineering, Chulalongkorn University
Bangkok 10330, Thailand
2 Department of Materials Science and Metallurgy, University of Cambridge,
Cambridge CB2 3QZ, UK
E-mail: fiespj@eng.chula.ac.th[1,*]

Abstract. The porous hydroxyapatite (HA) bioceramics were prepared through combination of sacrificial template and direct foaming techniques using PMMA granules (varied from 5 to 50wt% in content) as a template and H_2O_2 solution (varied from 5 to 30wt% in concentration) as a foaming agent, respectively. The effects of PMMA content and H_2O_2 concentration on final porosity, microstructure and mechanical strengths were studied. The porous samples using PMMA provided the porosity ranging from 52% to 75%, the samples using H_2O_2 had the porosity ranging from 82% to 85%, and the sample using both pore formers provided the porosity ranging between 84% and 90%. The higher content of PMMA and concentration of H_2O_2 led the porosity increased, leading to a decrease in the compressive and flexural strengths. Furthermore, this combination technique allowed interconnected pores having two levels of pore size, which came from PMMA and H_2O_2. The PMMA formed the small pores with the diameter ranging between 100 and 300 μm, while H_2O_2 provided the larger pores with the diameter ranging from 100 to 1,000 μm depending on concentration.

Keywords: Porous hydroxyapatite, fabrication, sacrificial template, direct foaming.

ENGINEERING JOURNAL Volume 15 Issue 2
Received 16 August 2010
Accepted 24 December 2010
Published 1 April 2011
Online at http://www.ej.eng.chula.ac.th/eng/
DOI:10.4186/ej.2011.15.2.1

1. Introduction

Nowadays, porous bioceramics have an increasingly important role in biomedical application, such as bone filler, orbital implant and drug delivery carriers [1]. One of the most popular topic focuses on porous hydroxyapatite (HA). Since it has a chemical composition ($Ca_{10}(PO_4)_6(OH)_2$) identical to human bone and an excellent biocompatibility. Moreover, porous structure provides outstanding bone ingrowths, vascularization and an increased interfacial area between the implant and the tissues resulting in the stronger attachment [1, 2, 3].

A number of pore forming techniques on bioceramics have been proposed, which can be classified into 3 main techniques [4]. There are (1) replica technique, e.g. replamineform and PU impregnation [5, 6]; (2) sacrificial template technique, e.g. starch consolidation, dual-phase mixing and camphene-based freeze casting [7, 8, 9]; and (3) direct foaming technique, e.g. foaming method and gelcasting [10, 11]. However, almost previous studies were based on using a single technique. A few works focused on porous fabrication using combination of these techniques. Padilla *et al.* studied on porous HA using combination of PU impregnation (replica) and gelcasting (direct foaming) techniques; and Batulli *et al.* studied on porous zirconia using polyethylene sphere as a sacrificial template and gelcasting techniques [12, 13]. In spite of these, it seems no study on fabrication of porous HA using combination of sacrificial template and direct foaming techniques.

The purpose of this study was to characterize the porous HA samples fabricated through combination of sacrificial template and direct foaming techniques using PMMA granules and H_2O_2 solution as a pore template and a foaming agent, respectively. Additionally, the effects of PMMA content and H_2O_2 concentration on the final porosity, microstructure, compressive strength and flexural strength of the samples were also investigated.

2. Materials and methods

2.1. Preparation of hydroxyapatite powder

A stoichiometric HA was prepared using the precipitation reaction between 0.5 moles calcium hydroxide (Riedel-de-Haen, Germany) and 0.3 moles orthophosphoric acid (Merck, Germany). The precipitation reaction was performed at room temperature and the pH was controlled at 10.5 by the addition of ammonium hydroxide solution (APS Finechem, Australia) [14]. During mixing process, the acid solution was slowly dropped into the vigorously stirring suspension, using a peristaltic pump [15]. After complete mixing of the reactants, the suspension was aged overnight. The precipitate was filtered, dried at 80^{o}C overnight and then ground to a powder by a pestle and mortar. Subsequently, the powder was sieved with the size of 100 μm.

2.2. Fabrication of porous hydroxyapatite

The poly-methyl-methacrylate granules (PMMA) being commercial grade was applied as a pore former for sacrificial template technique, while hydrogen peroxide solution, (H_2O_2) was used as a foaming agent for direct foaming technique.

The porous hydroxyapatite ceramics were prepared through three techniques, including sacrificial template, direct foaming and combination between sacrificial template and direct foaming. To fabricate the porous samples, the HA powder was homogeneously mixed with PMMA granule at various content (5, 10, 20, 30, 40 and 50wt%) and H_2O_2 solution at different concentration (5, 10, 20 and 30wt%), with the liquid to powder ratio (L/P ratio) of 1.3 ml/g. A series of sample name were listed in Table 1. To evaluate the effect of PMMA content and H_2O_2 concentration, the mixtures were prepared without addition of binder, deflocculant and other additives.

After mixing, the paste was placed into removable molds, and kept at 60^{o}C overnight. At this temperature, the decomposition of H_2O_2 produced the foaming of the paste. Afterwards, the green samples were removed from the molds and then heated at 400^{o}C for 1 hour with the slowly ramp rate of 1^{o}C/min for burning out PMMA granules and to avoid the cracking. Finally, the samples were sintered at 1100^{o}C for 2 hours with the ramp rate of 5^{o}C/min and then furnace cooled.

Table 1. The experimental plan layout and feasible production range of porous HA samples (Hxx-Pyy was referred to the sample produced with xx concentration (wt%) of H_2O_2 solution and yy content (wt%) of PMMA granule, and "X" was referred to the handleless sample).

H_2O_2 concentration (wt%)	PMMA content (wt%)						
	0	5	10	20	30	40	50
0	H00-P00	H00-P05	H00-P10	H00-P20	H00-P30	H00-P40	X
5	H05-P00	H05-P05	H05-P10	H05-P20	H05-P30	X	X
10	H10-P00	H10-P05	H10-P00	H10-P20	X	X	X
20	H20-P00	H20-P05	H20-P10	X	X	X	X
30	H30-P00	H30-P05	H30-P10	X	X	X	X

2.3. Characterizations

The Morphology of the synthesized HA powder and the as-received PMMA granule was characterized using laser particle size distribution analysis (LPD) and scanning electron microscope (SEM). In addition to the morphological study, SEM was also applied to observe the microstructure of the porous HA samples.

The phase purity of the sintered HA powder was analyzed using X-ray diffraction (XRD) with CuK_α radiation. The scanning range of 2θ was between 20^o and 50^o at the scan speed of 0.5^o/min.

The decomposition temperature of the PMMA granules was determined by thermo-gravimetric analysis (TGA) using simultaneous thermal analyzer (STA) with the heating rate of 10^oC/min.

The porosities of the sintered samples were calculated from the bulk density of the sample (ρ_{bulk}) and the theoretical density of hydroxyapatite (ρ_{HA} = 3.156 g/cm^3), by Eq (1).

$$Porosity = \left(1 - \frac{\rho_{bulk}}{\rho_{HA}}\right) \times 100\% \tag{1}$$

To examine the effect of PMMA content and H_2O_2 concentration on the porosity, the one-way analysis of variance (ANOVA) was performed at the significant level (α) of 0.05. In addition, such results were used to develop regression models to predict porosity.

The compressive strength and three-point flexural strength of porous HA samples were characterized according to ASTM C773-88 and C1161-02c specification, respectively.

3. Results and discussion

3.1. Characteristics of the HA powder and PMMA granule

Figure 1 showed particle size distribution of the HA powder and the PMMA granule. The distribution of the HA powder was a bimodal distribution with the peaks of approximately 4 μm and 20 μm in particle size, while that of the PMMA granules was an unimodal distribution with a peak of approximately 150 μm. The average and standard deviation of mean particle sizes of the both were summarized in Table 2. The average mean particle sizes of the HA powder and PMMA granules were 4.97±0.03 μm and 150.75±0.15 μm, respectively.

Figure 2 exhibited SEM micrographs of the HA powder and PMMA granules. In Fig. 2(a), the HA powder had angular particles with various sizes. This may be due to the manually milling process through a pestle and mortar. This is similar to the results from previous investigation by Gibson *et al* [14]. The larger particles appeared to be the agglomeration of smaller particles during sintering process. In Fig. 2(b), the PMMA granules obviously had a spherical shape with various sizes, ranged from 10 to 200 μm.

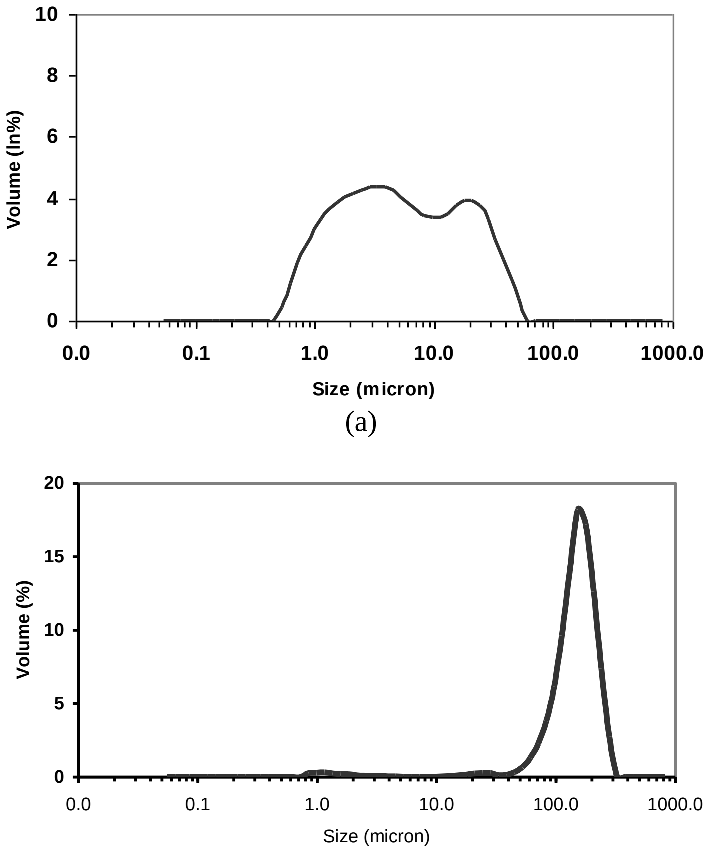

(a)

(b)

Fig. 1. Particle size distribution of (a) the HA powder and (b) PMMA granules.

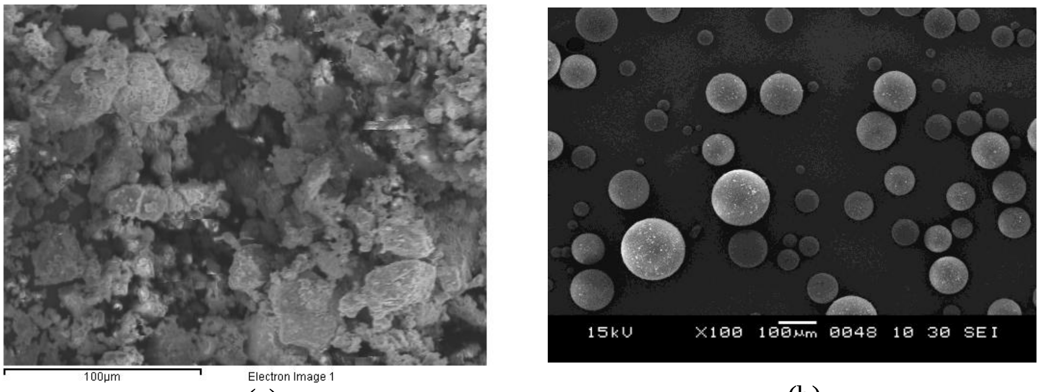

(a) (b)

Fig. 2. Particle morphology through SEM of (a) the HA particle sintered at 1100°C for 2 hr and (b) the as-received PMMA granules.

Figure 3 displayed XRD spectra of the HA powder sintered at 1100°C. The spectra showed the single phase of HA, corresponding to the ICDD standard peak of stoichiometric hydroxyapatite (standard No.09-0432). Furthermore, this result agrees with a previous study in that sintering at high temperature resulted in the sharp and narrow diffraction peaks [16].

Figure 4 illustrated TGA curve of the as-received PMMA granules. A stable weight was attained at about 400°C, which indicates that the PMMA granules have been completely decomposed at about 400°C. This results is similar to the previous report by Yao *et al* [17]. In order to let PMMA decompose completely and avoid the cracks in HA ceramics, the heating rate of the green HA body should be very slow at sintering temperature below 400°C. This is why the heating rate of the samples was set at 1°C/min.

Table 2. Average and standard deviation of particle sizes of the prepared HA powders and the as-received PMMA granules (d0.1, d0.5 and d0.9 were referred to the measured particle size of diameter at 10, 50 and 90Vol% of the powder particles).

Type	Particle size (μm)		
	d0.1	d0.5	d0.9
HA powder	1.12 ± 0.01	4.97 ± 0.03	26.31 ± 0.19
PMMA granule	82.69 ± 0.27	150.75 ± 0.15	222.95 ± 0.49

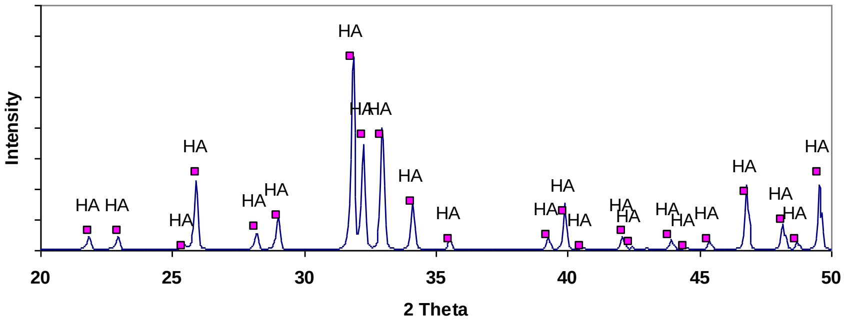

Fig. 3. XRD spectra of the synthesized HA powder sintered at 1100°C for 2 h.

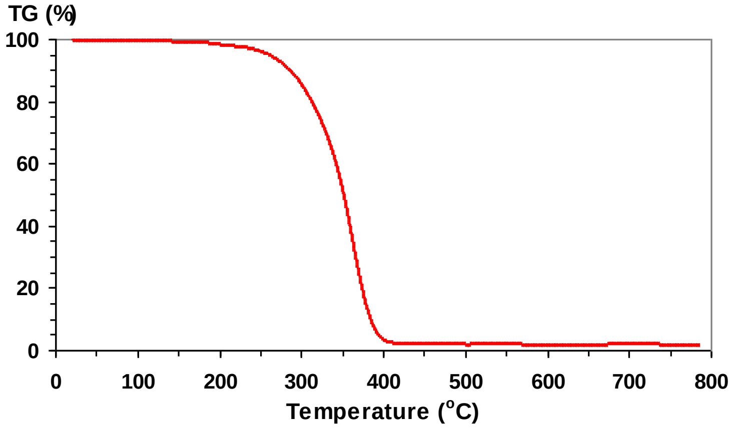

Fig. 4. TGA curve of the as-received PMMA granules.

3.2. Effect of PMMA and H_2O_2 on porosity

Table 1 showed the feasible production range of the porous HA samples in this study. The samples prepared using only PMMA at the content of over 40wt% were handless, while the samples mixed with H_2O_2 solution at the concentration of over 20wt% were very brittle. To prepare the samples using both PMMA and H_2O_2, a balance between the PMMA content and the H_2O_2 concentration must be considered as shown in Table 1.

Figure 5 presented effect of PMMA content and H_2O_2 concentration on porosity of the HA samples performed by various techniques: (a) sacrificial template; (b) direct foaming; and (c) combination between sacrificial and direct foaming. Table 3 summarized P-value from analysis of variance (ANOVA) for porosity of the porous HA samples prepared by various forming methods (at $\alpha = 0.05$).

Table 4 listed the regression models and R-square values from regression analysis for porosity of the porous HA samples prepared by various methods.

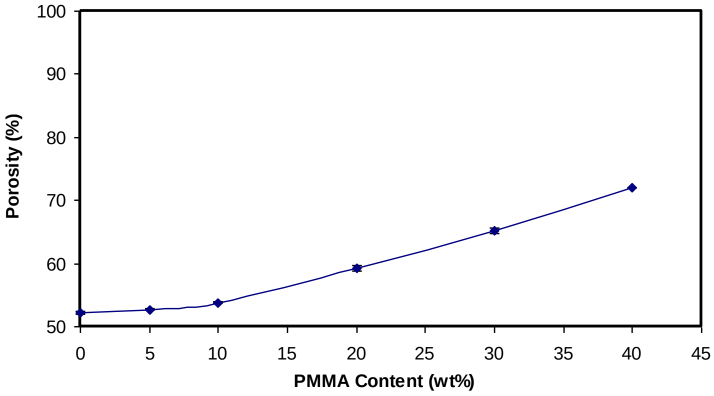

(a) Sacrificial template using PMMA

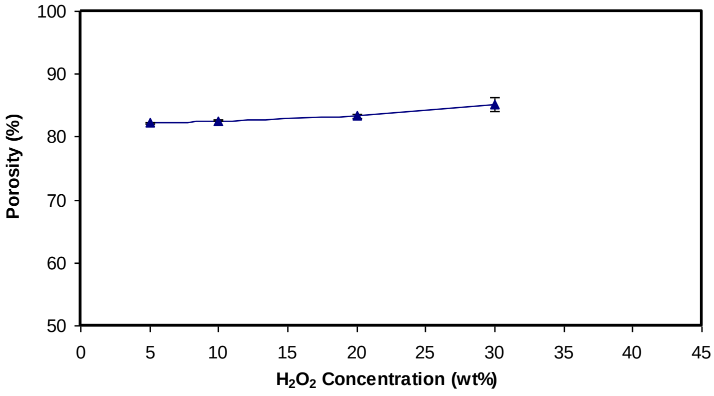

(b) Direct foaming using H_2O_2

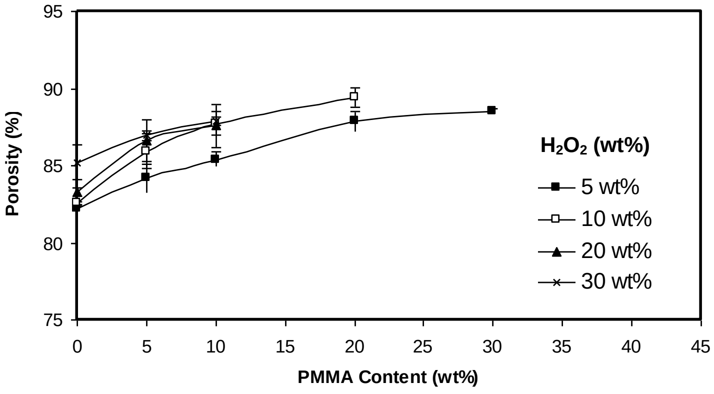

(c) Combination technique using PMMA and H_2O_2

Fig. 5. Effect of PMMA content and H_2O_2 concentration on porosity of the HA sample performed by various techniques: (a) sacrificial template using PMMA, (b) direct foaming using H_2O_2, and (c) combination technique using PMMA and H_2O_2.

Figure 5(a) showed the final porosity of the specimens using PMMA granules as pore template. The porosity of the HA sample (H00-P00) was approximately 52%. Obviously, the porosity increased with an increasing content of PMMA used. This result agreed with a previous study by Yao *et al* [17]. By this technique, the porosity reached approximately 75% at the PMMA content of 40wt%. The relation between the porosity (P) and the content of PMMA (C_P) was explained by the regression model (1) in Table 4

Figure 5(b) exhibited the porosity of the samples using H_2O_2 solution as pore former. The porosity of the samples increased slightly from ~82% up to ~85%, when the concentration of H_2O_2 increased from 5wt% to 30wt%. To confirm the effect of H_2O_2 concentration on porosity, ANOVA test was performed. This statistical analysis confirmed that the concentration of hydrogen peroxide had a significant effect on porosity, with the P-value of 0.022, at 95% confident interval, as shown in Table 3. Furthermore, the porosity of the samples using H_2O_2 less than 5wt% could be predicted by the regression model (2) in Table 4. However, compared to the sample H00-P00, adding H_2O_2 (5wt%) resulted in a dramatic increase in porosity of about 30%. This was because the addition of H_2O_2 into ceramic slurry produced gas voids when it was stored at 60^{o}C, although a small amount of H_2O_2 was applied [10]. At elevated temperature, H_2O_2 could produce H_2 and O_2 gases, leading to the voids in ceramic bodies. The gas voids were driven out by heating during the liquid phase. After drying process, the gas voids remaining in the paste became the pores in porous dry bodies.

Figure 5(c) illustrated the porosity of the porous samples prepared through combination technique using PMMA granule and H_2O_2 solution. It seemed a minor change in porosity was found, when both PMMA content and H_2O_2 concentration increased. From P-values in Table 3, the content of PMMA had a significant effect on porosity when the H_2O_2 concentration was at 5wt% and 10wt%, with the P-value of 0.001 and 0.003, respectively (at 95% confident interval). However, at 20wt% and 30wt% H_2O_2, the PMMA content showed an insignificant effect on porosity with the P-value of 0.066 and 0.061, respectively (at 95% confident interval). As expected, the samples using H_2O_2 with the concentration of over 20 wt% were hard to be prepared. So, mixing PMMA into these samples had barely affected on porosity. The porosity of the samples using both PMMA and H_2O_2 could be estimated by the regression model (3) in Table 4.

From above results, it seemed that the porosity derived from PMMA granules was dominated by H_2O_2 solution. This was because PMMA granule formed pores by decomposition at above 400^{o}C in solid state while H_2O_2 produced pores by expansion of gas voids in liquid phase, which provide the higher porosity than PMMA.

Table 3. Analysis of variance for porosity of the porous HA samples prepared by various methods (at $\alpha = 0.05$).

Method	Factor	P-value
1. Sacrificial template using PMMA	Content of PMMA	< 0.001
2. Direct foaming using H_2O_2	Concentration of H_2O_2	0.022
3. Combination technique using PMMA and H_2O_2		
3.1. at 5wt% H_2O_2	Content of PMMA	0.001
3.2. at 10wt% H_2O_2	Content of PMMA	0.003
3.3. at 20wt% H_2O_2	Content of PMMA	0.066
3.4. at 30wt% H_2O_2	Content of PMMA	0.061

Table 4. Regression analysis of the porous HA samples prepared by various methods (P was referred to the expected porosity (%), C_P was referred to the content of PMMA (wt%), and C_H was referred to the concentration of H_2O_2 (wt%), respectively).

Method	Regression Model		R-square
1. Sacrificial template using PMMA	(1) $P = 0.008C_P^2 + 0.204C_P + 51.716$	; $0 \le C_P \le 40$	0.9960
2. Direct foaming using H_2O_2	(2) $P = 0.004C_H^{2} - 0.038C_H + 82.387$	; $0 < C_H \le 30$	0.8855
3. Combination technique using PMMA and H_2O_2	(3) $P = -0.012C_P^2 + 0.538C_P + 0.298C_H + 80.2$	; $0 \le C_P \le 20$; $0 < C_H \le 10$	0.9350

3.3. Effect of PMMA and H_2O_2 on microstructure

Figure 6 illustrated SEM micrographs of the HA samples prepared with different conditions, after sintering at 1100°C for 2 hours. The sintered HA or the sample of H00-P00 had a few small pores with less than 50 μm in diameter, as shown in Fig. 6(a). These pores were derived from driving out of water during drying process.

The porous samples prepared by 10wt% and 30wt% PMMA content were presented in Fig. 6(b) and 6(c), respectively. From the samples, they were composed of two groups of pore size range. The large pore group had the diameter range of 100-300 μm, arising from PMMA granules, which conformed to the particle size measured and corresponded to Yao *et al* [17]. However, it seemed that the small pore group had a similar pore size as seen in the H00-P00 sample. Moreover, the more content of PMMA the higher amount of pores.

The porous samples prepared using 10wt% and 20wt% H_2O_2 concentration were shown in Fig. 6(d) and Fig. 6(e), respectively. By direct foaming technique, the samples had a number of pores with the diameter larger than 100 μm. Comparison between the sample H10-P00 and H20-P00 indicated that the amount of pores and pore size were increased when using a higher concentration of H_2O_2. However, it seemed there were a few pores derived from water. This result is agree with a previous study by Almirall *et al* [10].

The HA sample prepared through combination technique using 10wt% PMMA content and 10wt% H_2O_2 concentration was displayed in Fig. 6(f). It seemed that the sample consisted of the large pores in the ceramic body and the small pores in the ceramic wall. The large pore size was up to 1000 μm in diameter, while small pore size ranged between 100 and 300 μm in diameter. The large pores were possibly resulted from H_2O_2, while small pores might be from PMMA granules. Moreover, the interconnected pores were observed. The interconnected pores, pathways between pores, conduct cells and vessels between pores and thus favor bone ingrowth inside ceramics [18].

Based on previous studies, the minimum requirement for pore size is considered to be ~ 100 μm due to cell size, migration requirements and transport. However, pore sizes over 300 μm was favorable to enhanced new bone formation and cell regeneration [18, 19]. Therefore, the sample prepared by combination technique using both PMMA and H_2O_2 can provide the pores attaining these requirements.

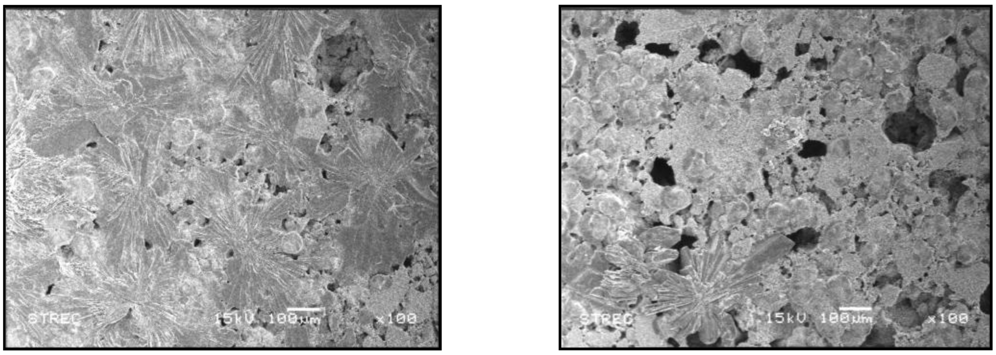

(a) H00-P00 (b) H00-P10

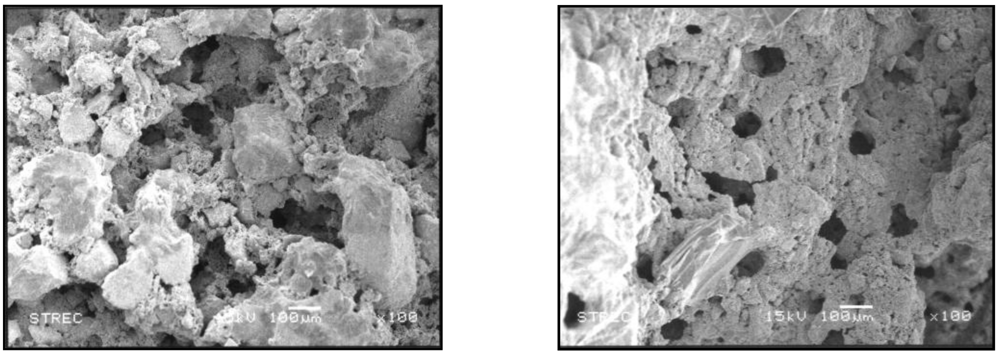

(c) H00-P30 (d) H10-P00

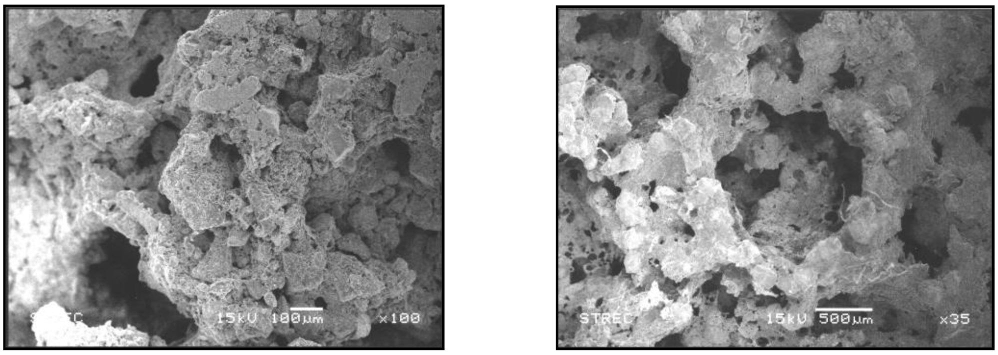

(e) H20-P00 (f) H10-P10

Fig. 6. SEM micrographs of the sintered HA samples prepared with different conditions: (a) H00-P00, (b) H00-P10, (c) H00-P30, (d) H10-P00, (e) H20-P00 and (f) H10-P10.

3.4. Effect of PMMA and H_2O_2 on mechanical strength

Figure 7 showed the effect of PMMA content and H_2O_2 concentration on compressive strength of the HA samples performed by sacrificial template, direct foaming and combination between sacrificial template and direct foaming. In Fig. 7(a), the compressive strength of the samples prepared using PMMA granules dropped from approximately 25 MPa to 0.6 MPa when the template content used increased from 5wt% to 40wt%, while the HA cement (H00-P00) had the compressive strength of around 35 MPa. In Fig. 7(b), the compressive strength of the samples prepared using H_2O_2 solution decreased from approximately 0.3 MPa to 0.15 MPa when concentration of the foaming agent was increased from 5wt% to 30wt%. Compared to the sample H00-P00, an addition of H_2O_2 could affect on falling in compressive strength of the HA samples due to a dramatic increase in porosity [10]. Also, it seemed that H_2O_2 has a more influence on impairing the strength than PMMA, because H_2O_2 could cause higher porosity than PMMA. In Fig. 7(c), the samples prepared through combination technique showed a decrease in compressive strength when using higher PMMA content and higher concentration of H_2O_2. In other words, the compressive strength decreases with an increase of final porosity.

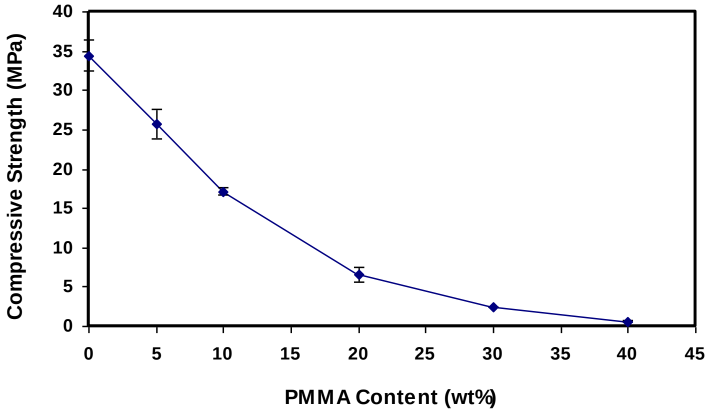

(a) Sacrificial template using PMMA

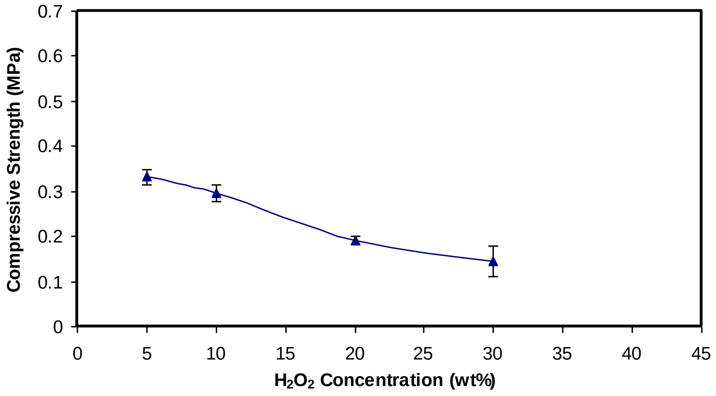

(b) Direct foaming using H_2O_2

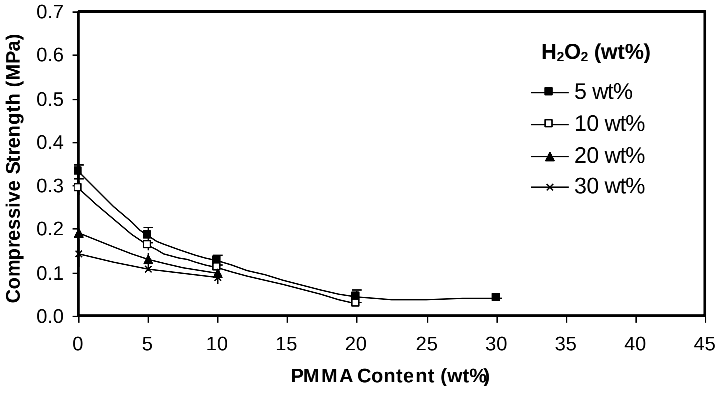

(c) Combination technique using PMMA and H_2O_2

Fig. 7. Effect of PMMA content and H_2O_2 concentration on compressive strength of the HA samples performed by various techniques: (a) sacrificial template using PMMA, (b) direct foaming using H_2O_2, and (c) combination technique using PMMA and H_2O_2.

Figure 8 exhibited the effect of PMMA content and H_2O_2 concentration on flexural strength of the HA samples performed by sacrificial template, direct foaming and combination between both techniques. The flexural strength of the specimens prepared using PMMA decreased from around 5.5 MPa to 0.7 MPa when the content of the pore template was raised from 5wt% to 40wt%, as shown in

Fig. 8(a). The flexural strength of the specimens prepared using H_2O_2 was diminished from approximately 0.5 MPa to 0.2 MPa when concentration of the foaming agent increased from 5wt% to 30wt%, as illustrated in Fig. 8(b). As expect, this result is consistent with the compressive strength in that H_2O_2 had a more effect than PMMA on the strength. Finally, the specimens prepared through combination technique had a decrease in flexural strength when higher content of PMMA and higher concentration of H_2O_2 were added.

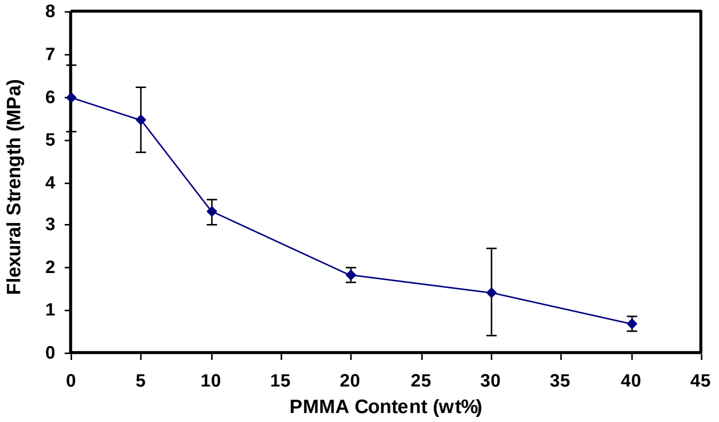

(a) Sacrificial template using PMMA

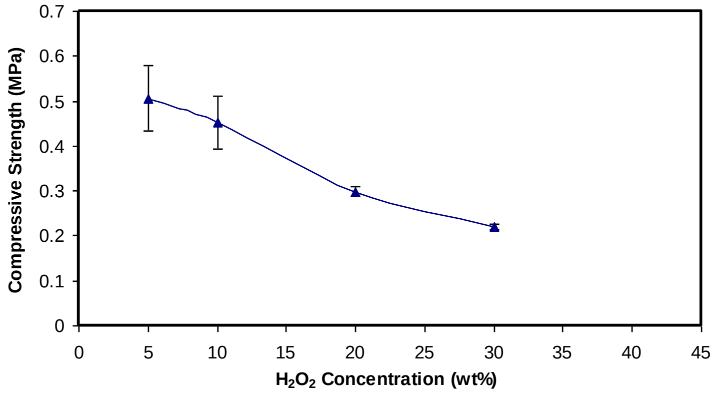

(b) Direct foaming using H_2O_2

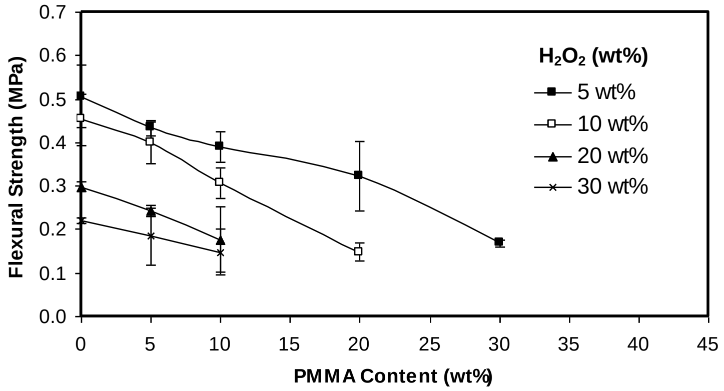

(c) Combination technique using PMMA and H_2O_2

Fig. 8. Effect of PMMA content and H_2O_2 concentration on flexural strength of the HA samples performed by various techniques: (a) sacrificial template using PMMA, (b) direct foaming using H_2O_2, and (c) combination technique using PMMA and H_2O_2.

Figure 9 and Figure 10 presented the effect of porosity on compressive strength and flexural strength, respectively, of the HA samples divided by forming technique, including sacrificial template using PMMA, direct foaming using H_2O_2, combination technique using PMMA and H_2O_2, and overall techniques.

The samples prepared through sacrificial template using PMMA provided the widest range of mechanical strengths (35 to ~1 MPa in compressive strength and 6 to ~1 MPa in flexural strength), as shown in Fig. 9(a) and Fig. 10(a).

The samples prepared by direct foaming using H_2O_2 showed a decrease in both strengths (from 0.3 to ~0.1 MPa in compressive strength and from ~0.5 to 0.2 MPa in flexural strength) when porosity increased, as illustrated in Fig. 9(b) and Fig. 10(b).

The samples using both PMMA and H_2O_2 also had a decrease in mechanical strengths (~0.2-0.05 MPa in compressive strength and 0.4-0.1 MPa in flexural strength) when porosity rose, as exhibited in Fig. 9(c) and Fig. 10(c).

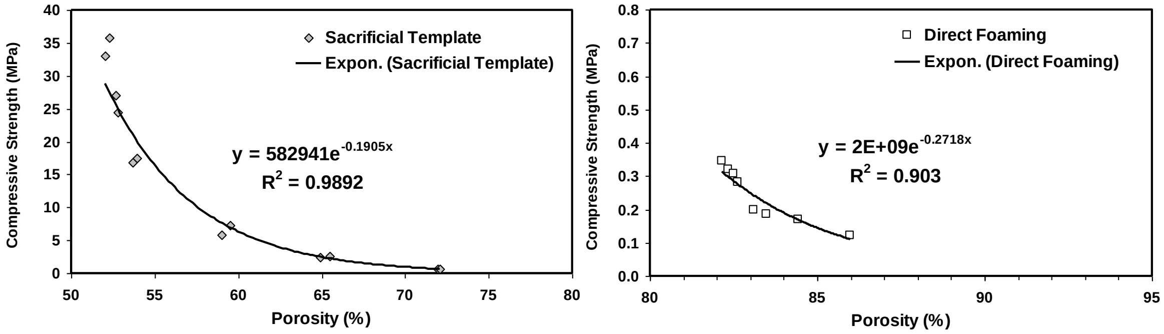

(a) Sacrificial template using PMMA

(b) Direct foaming using H_2O_2

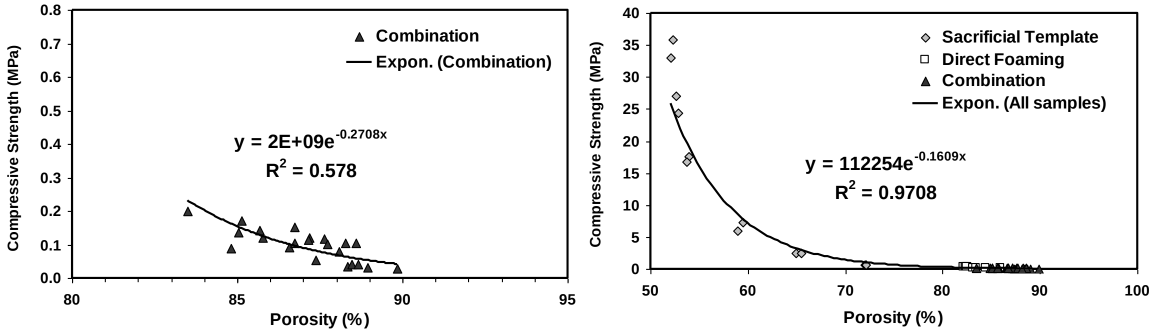

(c) Combination technique using PMMA and H_2O_2

(d) Overall

Fig. 9. Effect of Porosity on compressive strength of the porous HA samples divided by forming techniques: (a) sacrificial template using PMMA, (b) direct foaming using H_2O_2, (c) combination technique using PMMA and H_2O_2 and (d) overall technique.

It seemed that both compressive strength and flexural strength decreased with an increasing porosity for all forming techniques, as summarized in Fig. 9(d) and Fig. 10(d). These results agreed with previous research that the mechanical strength of the sample was conversely relative to the amount of pore former used and final porosity [9, 10, 17]. Furthermore, the samples with the porosity higher than 80% showed a fluctuation in strength, particularly flexural strength. On the other hand, the samples using H_2O_2 (i.e. direct foaming and combination technique) provided high variation in strength more than those using PMMA. This was because the porosity obtained from H_2O_2 could not be effectively controlled.

Nevertheless, the mechanical strengths of the samples in this study were lower than the minimum strength of cancellous bone. The minimum compressive strength and flexural strength of human cancellous bone were approximately 2 MPa and 10 MPa, respectively [20]. The pore size favorable to bone formation and cell regeneration was over 300 μm [19]. As well as the interconnected pores favors to cell ingrowth inside the pore [18]. But, there are no report on suitable porosity for these applications. As a result, such samples were not applicable for a scaffold in bone restoration due to the lack of strength. However, these materials could be applied for fabrication of an eye ball in orbital implant being porous bioceramics.

Furthermore, the low mechanical strengths of porous hydroxyapatite prepared by this combination technique using PMMA and H_2O_2 could be developed by adding some additives; such as binder, deflocculant or surfactant. Additionally, using hydrogen peroxide less than 5wt% concentration might be another way to improve the strength of the porous samples.

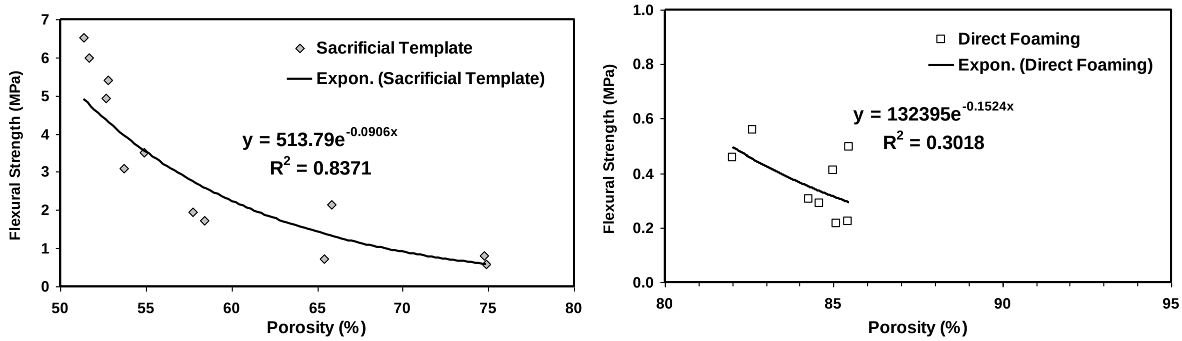

(a) Sacrificial template using PMMA

(b) Direct foaming using H_2O_2

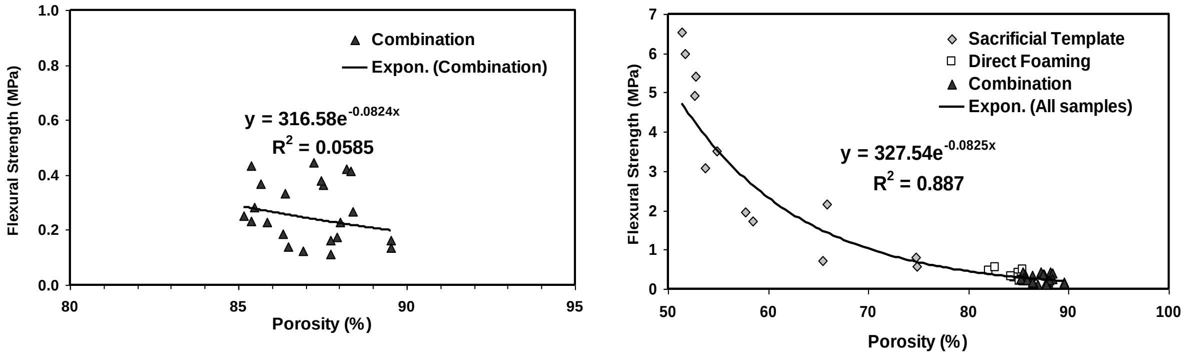

(c) Combination technique using PMMA and H_2O_2

(d) Overall

Fig. 10. Effect of Porosity on flexural strength of the porous HA samples divided by forming techniques: (a) sacrificial template using PMMA, (b) direct foaming using H_2O_2, (c) combination technique using PMMA and H_2O_2 and (d) overall technique.

4. Conclusion

This study investigated the characteristics of the porous HA prepared by three different methods and the effect of pore former on their mechanical properties, summarized as follows:

(1) An increasing porosity of the hydroxyapatite samples resulted in a decrease of both compressive strength and flexural strength.

(2) For sacrificial template, the more PMMA content had a significant effect on the higher porosity of the HA samples whereas the lower compressive strength and flexural strength. These samples had the pore size ranged between 100 and 300 μm.

(3) For direct foaming, the higher concentration of H_2O_2 resulted in an increase in porosity and pore size, while a decrease in the both mechanical strength. The pore size of these samples ranged from 100 to 1000 μm.

(4) There were hard to prepare the porous HA using PMMA content over 40wt% for sacrificial template and H_2O_2 concentration over 20wt% for direct foaming when L/P ratio was controlled at 1.3 ml/g.

(5) For combination between sacrificial template and direct foaming, an increasing use of PMMA and H_2O_2 caused a rise in porosity and a drop in both compressive and flexural strengths.

(6) The HA samples prepared through sacrificial template provided the porosity ranged between 52% and 75%, while the samples produced by direct foaming and combination technique provided the porosities ranged from 82% to 85% and from 84% to 90%, respectively.

5. Acknowledgement

The authors would like to thank the Graduate School and Department of Industrial Engineering, Faculty of Engineering, Chulalongkorn University for financial support and also Department of Material Science and Metallurgy, University of Cambridge for laboratory cooperation.

References

[1] H. Aoki, *Medical Applications of Hydroxyapatite*: Takayama Press, 1994.

[2] L. L. Hench, "Bioceramics," *Journal of the American Ceramic Society,* vol. 81, pp. 1705-1728, 1998.

[3] S. W. K. Kweh, K. A. Khor, and P. Cheang, "The production and characterization of hydroxyapatite (HA) powders," *Journal of Materials Processing Technology,* vol. 89-90, pp. 373-377, 1999.

[4] A. R. Studart, U. T. Gonzenbach, E. Tervoort, and L. J. Gauckler, "Processing routes to macroporous ceramics: a review," *Journal of the American Ceramic Society,* vol. 89, pp. 1771-1789, 2006.

[5] D. C. Tancred, B. A. O. McCormack, and A. J. Carr, "A synthetic bone implant macroscopically identical to cancellous bone," *Biomaterials,* vol. 19, pp. 2303-2311, 1998.

[6] S.-H. Kwon, Y.-K. Jun, and S.-H. Hong, "Calcium phosphate bioceramics with various porosities and dissolution rates," *Journal of the American Ceramic Society,* vol. 85, pp. 3129-31, December 2002.

[7] L. M. Rodriguez-Lorezo, J. Ferreira, and M. Vallet-Regí, "Processing of porous hydroxyapatite by starch consolidation," *Bioceramics,* vol. 11, pp. 89-92, 1998.

[8] S. H. Li, J. R. de Wijn, and P. Layrolle, "Novel method to manufacture porous hydroxyapatite by dual-phase mixing," *Journal of the American Ceramic Society,* vol. 86, pp. 65-72, January 2003.

[9] E. J. Lee, Y. H. Koh, B. H. Yoon, H. E. Kim, and H. W. Kim, "Highly porous hydroxyapatite bioceramics with interconnected pore channels using camphene-based freeze casting," *Materials Letters,* vol. 61, pp. 2270-2273, 2007.

[10] A. Almirall, G. Larrecq, J. A. Delgado, S. Martínez, J. A. Planell, and M. P. Ginebra, "Fabrication of low temperature macroporous hydroxyapatite scaffolds by foaming and hydrolysis of an α-TCP paste," *Biomaterials,* vol. 25, pp. 3671-3680, 2004.

[11] P. Sepulveda, F. S. Ortega, M. D. M. Innocentini, V. C. Pandolfelli, and D. Green, "Properties of highly porous hydroxyapatite obtained by the gelcasting of foams," *Journal of the American Ceramic Society,* vol. 83, p. 3021, 2000.

[12] S. Padilla, J. Romàn, and M. Vallet-Regí, "Synthesis of porous hydroxyapatites by combination of gelcasting and foams burn out methods," *Journal of Materials Science: Materials in Medicine,* vol. 13, pp. 1193-1197, 2002.

[13] C. Bartuli, E. Bemporad, J. M. Tulliani, J. Tirillò, G. Pulci, and M. Sebastiani, "Mechanical properties of cellular ceramics obtained by gel casting: Characterization and modeling," *Journal of the European Ceramic Society*, vol. 29, pp. 2979-2989, 2009.

[14] I. R. Gibson, S. Ke, S. M. Best, and W. Bonfield, "Effect of powder characteristics on the sinterability of hydroxyapatite powders," *Journal of Materials Science: Materials in Medicine,* vol. 12, pp. 163-171, 2001.

[15] E. Bouyer, F. Gitzhofer, and M. I. Boulos, "Morphological study of hydroxyapatite nanocrystal suspension," *Journal of Materials Science: Materials in Medicine,* vol. 11, pp. 523-531, 2000.

[16] N. Patel, I. R. Gibson, S. Ke, S. M. Best, and W. Bonfield, "Calcining influence on the powder properties of hydroxyapatite," *Journal of Materials Science: Materials in Medicine,* vol. 12, pp. 181-188, 2001.

[17] X. Yao, S. Tan, and D. Jiang, "Improving the properties of porous hydroxyapatite ceramics by fabricating methods," *Journal of Materials Science,* vol. 40, pp. 4939-4942, 2005.

[18] J. X. Lu, B. Flautre, K. Anselme, P. Hardouin, A. Gallur, M. Descamps, and B. Thierry, "Role of interconnections in porous bioceramics on bone recolonization in vitro and in vivo," *Journal of Materials Science: Materials in Medicine,* vol. 10, pp. 111-120, 1999.

[19] V. Karageorgiou and D. Kaplan, "Porosity of 3D biomaterial scaffolds and osteogenesis," *Biomaterials,* vol. 26, pp. 5474-5491, 2005.

[20] A. A. White, S. M. Best, and I. A. Kinloch, "Hydroxyapatite-carbon nanotube composites for biomedical applications: A review," *International Journal of Applied Ceramic Technology,* vol. 4, pp. 1-13, 2007.